

mobilization and neoplastic transformation[4]. However, HepG2 is aberrant expression of connexin protein and is deficient in GJIC. In the liver, connexin32 (Cx32) is the major gap junction protein expressed in hepatocytes, therefore, the aim of this study is focused on enhancing GJIC and improving liver-specific functions of HepG2 by Cx32 gene transfection.

Key word: Bioartificial liver, Connexin, Hepatoma cell

## 2. Materials and Methods

### 2.1. Cell culture

The human hepatoma cell lines HepG2 from the Riken cell bank (Tokyo, Japan) was cultured at 37°C under 5% CO<sub>2</sub> / 95% humidified air using Minimum Essential Medium (MEM) (Nissui Pharmaceutical Co., Ltd., Tokyo, Japan) containing 0.1mM non-essential amino acids (NEAA) (Gibco), 10% fetal bovine serum (FBS) (Intergen Co., NY.) and 100U/ml Penicillin-Streptomycin (Gibco).

### 2.2. Plasmid construction and transfection

The connexin gene fragments amplified by polymerase chain reaction were isolated and inserted into the pTARGET™ mammalian expression system. HepG2 cells were transfected with the Cx/pTARGET™ plasmid DNA using FuGENE6 transfection reagent according to manufacturer's instruction with minor modification, cells transfected with empty vector as a control. After continuously culturing for two days, transfectants were selected by adding geneticin (Life Technologies, Inc., Frederick, MD) in the culture medium for one week. Individual transfected clones were prepared by limiting dilution cloning in 96-well plates, and then cultured as same as the HepG2.

### 2.3. Immunocytochemical stainings

Immunocytochemical staining of Cx32 protein was performed using the VECTASTAIN ABC kit in manufacturer's instruction with some modification. Briefly, cells grown on the glass cover slips were fixed in cold pure acetone for 5 min. The acetone-fixed specimens were blocked in diluted normal blocking serum in Dulbecco's phosphate buffered saline (PBS) at room temperature for 30min, and incubated with polyclonal rabbit anti-connexin32 (Zymed Laboratories Inc., San Francisco, CA) over night at 4 °C . Protein-antibody complexes were visualized by the biotin/streptoavidin/oxidase method with diaminobenzidine tetrahydrochloride (DAB) as the chromogen (Vectox Laboratories, Burlingame, USA). All slides were viewed with a Nikon microscope (Nikon, Japan).

#### *2.4. Scrape-loading dye transfer (SLDT) assay for measurement of GJIC*

The SLDT technique was adapted after the method of E1-Fouly et al. [5]. Briefly, when the cells grew into confluent monolayer cells in 35-cm dishes; cell dishes were loaded with 0.05% Lucifer Yellow (Molecular Probes, Eugene, OR, USA) in PBS (+) solution and were scraped immediately with a sharp blade after rinsing with PBS (+). Then incubating for 5 min at 37°C, cells were washed with PBS (+) and monitored using fluorescence microscope. The distance of the dye spreading was measured from the cell layer at the scrape to the edge of the dye front that was visually detectable.

#### *2.5. Liver-specific function assay*

The functions of the HepG2 and Cx32 transfected cells were evaluated by measuring ammonia removal and albumin secretion. For the ammonia removal activities of these cells, the cells were cultured in MEM medium with 5mM ammonium chloride. After the exchange of the medium containing ammonium, the concentration of ammonia in the medium was measured at 0 and 24hrs, respectively, using the indophenol method (an ammonia assay kit, Wako Pure Chem., Japan).

#### *2.6. Statistical analysis*

Student's t-test was used to compare the samples. Statistical significance was represented by  $p < 0.05$ . Data were indicated as the mean  $\pm$  S.D (Standard Deviation). Three cultures were run for each case, and all experiments were repeated at least twice.

### **3. Results and Discussion**

#### *3.1. Functional GJIC in HepG2 enhanced by Cx32 gene transfection*

HepG2 cells were transfected with Cx32/pTARGET™ plasmid DNA using FuGENE6 transfection reagent, and the transfectants were obtained by selection with geneticin. Enhanced expression of Cx32 mRNA was confirmed by RT-PCR (date not shown). The abilities of GJIC in Cx32 plasmid DNA transfectants were investigated by the scrape-loading dye transfer technique. Lucifer yellow, a molecular probe with low molecular weight, can diffuse in the neighboring cells through the gap junction, but not transmits from intact plasma membranes. Therefore, the transfer distances of lucifer yellow reflect the functional GJIC in the cells, and the longer distance shows the higher functional GJIC in the cells. The transfer distance of lucifer yellow in Cx32 gene transfected cells was longer than those of HepG2 and empty vector transfected cells. Thus, the distance in Cx32 gene transfected cells was 2.8 times and 2 times as long as that of HepG2 and empty vector transfected cells, respectively. It could be concluded

that the functional GJIC in HepG2 was significantly enhanced by the Cx32 gene transfection.

### 3.2. Localization of Cx32 protein before and after Cx32 gene transfection

In order to confirm the contribution of Cx32 proteins for the formation of functional GJIC after the Cx32 gene transfection, the localizations of Cx32 protein in the cells were further observed by immunocytochemical staining (Fig.1). The results demonstrated that the Cx32 protein expressed in HepG2, Cx32 gene transfected cells

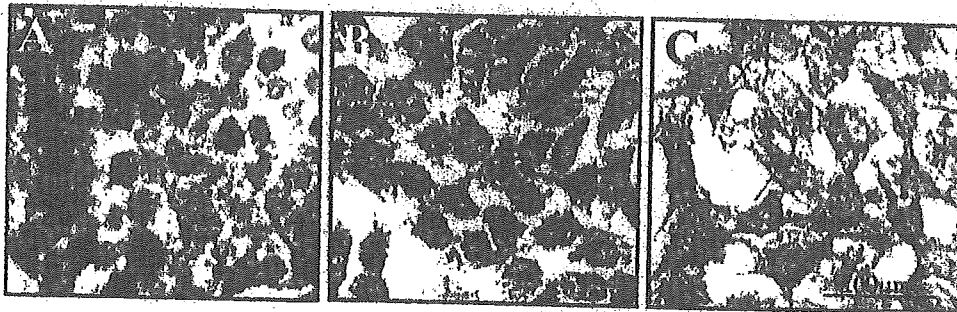


Fig.1. Immunocytochemical staining for Cx32 in HepG2 (A), empty vector transfected cells (B) and Cx32 gene transfected cells (C).

and empty vector transfected cells, but the localizations of Cx32 protein were obviously different among them. Thus, the Cx32 protein was localized in the cell borders and formed many small gap junction plaques in the neighboring cells transfected with Cx32 gene (Fig.1.C), however, the Cx32 protein was limited in the cytoplasm and hardly detected the gap junction plaques in the HepG2 (Fig.1.A) and empty vector transfected cells (Fig.1.B). Furthermore, the morphologies of the cells showed that Cx32 gene transfected cells grew as a monolayer with the spreading cell shape, whereas the HepG2 grew as the clusters with the spherical cell shape. Although the precise role of the cellular morphology in gap junctional channel formation between the cells is not clear at the present, the results in our study could be concluded that the traffic of Cx32 protein to the cell membrane in HepG2 was enhanced by Cx32 gene transfection and then increased the GJIC in Cx32 gene transfected cells.

### 3.3. Liver-specific function in HepG2 improved by Cx32 gene transfection

For determining the effect of Cx32 gene transfection on the liver-specific function in HepG2, the ammonia removal activity were continuously monitored in the HepG2, empty vector transfected cells and Cx32 gene transfected cells, respectively. Ammonia clearance, which represents the detoxification potentiality of liver, was significantly higher in the Cx32 gene transfected cells than HepG2 and empty vector transfected cells

uring the 14 days. These results showed that the ammonium metabolic activity in HepG2 related with the functional gap junctional channel composed of Cx32 proteins. It was considered that the small molecular ammonium was effectively eliminated through the gap junctional channels improved by Cx32 gene transfection in HepG2.

In conclusion, transfection of Cx32 gene increased the functional GJIC in HepG2 and enhance the activity of detoxification in the Cx32 gene transfected HepG2. It may be expected to improve the cellular function of the hepatoma cell line by Cx32 gene transfection and serve to develop an excellent biohybrid-artificial liver.

#### References:

Sussman NL, Gislason GT, Conlin CA, Kelly JH (1994) The hepatic extracorporeal liver assist device-initial clinical experience. *Artif Organs* 18:390-396.

Yamashita Y, Shimada M, Tsujita E, Tanaka S, Ijima H, Nakazawa K, Sakiyama R, Fukuda J, Ueda T, Funatsu K, Sugimachi K. (2001) Polyurethane foam/spheroid culture system using human hepatoblastoma cell line (HepG2) as a possible new hybrid artificial liver. *Cell Transplantation* 10:717-722.

Takagi M, Fukuda N, Yoshida T. (1997) Comparison of different hepatocyte cell lines for use in a hybrid artificial liver model. *Cytotechnology* 24:39-45.

Marie PP, Rosanne MT, Martha JF, Robert DB, Randall JR. (2000) Liver cell-specific transcriptional regulation of connexin 32. *Biochimica et Biophysica Acta* 1491:107-122.

El-Fouly MH, Trosko JE, Chang CC. (1987) Scrape-loading and transfer: A rapid and simple technique to study gap junctional intercellular communication. *Exp. Cell Res.* 168:422-430.

# Effects of Multipurpose Solutions (MPS) for Hydrogel Contact Lenses on Gap-Junctional Intercellular Communication (GJIC) in Rabbit Corneal Keratocytes

Taizo Sumide, Toshie Tsuchiya

Division of Medical Devices, National Institute of Health Sciences, 1-18-1, Kamiyoga, Setagaya-ku, Tokyo 158-8501, Japan

Received 9 January 2002; revised 15 July 2002; accepted 25 July 2002

Published online 13 December 2002 in Wiley InterScience (www.interscience.wiley.com). DOI: 10.1002/jbm.b.10510

**Abstract:** To ensure the effects of multipurpose solutions (MPS) for hydrogel contact lenses on the cornea, the inhibitory activity of three types of MPS on corneal cells has been evaluated with the use of scrape loading and dye transfer assay (SLDT assay) and Western blotting on rabbit corneal keratocytes (RC4). In SLDT assay, MPS-A and poloxamine showed dose-dependent inhibitory activity, suggesting the inhibitory action of MPS-A and poloxamine to gap junctional intercellular communication (GJIC) in the tested cells. Moreover, after treatment with MPS-A, the GJIC was initially inhibited within 4 h, and thereafter gradually turned to an approximately 60% level of the initial value. When MPS-A was removed from the incubation media after exposure of the cells, the recovery of GJIC was time dependent and returned to approximately initial levels at 8 h. Complete recovery was established after approximately 24 h. These findings suggested that the inhibitory action of MPS-A on corneal keratocytes was reversible. This inhibition was accompanied by a decrease in the quantity of connexin-43, which is a major protein constituting the gap junctional channel of these cells, and its change in the phosphorylation state. Taken together, it was suggested that MPS-A interacts with connexin-43, inducing an inhibitory action on GJIC. © 2002 Wiley Periodicals, Inc. *J Biomed Mater Res Part B: Appl Biomater* 64B: 57–64, 2003

**Keywords:** multipurpose solution (MPS); gap junctional intercellular communication (GJIC); metabolic cooperation assay (MC assay); scrape loading and dye transfer (SLDT assay); connexin-43

## INTRODUCTION

The use of contact lenses has gained popularity due to the comfort and convenience of lens wear. Contact lenses are medical devices that require proper care for safe use. Most complications associated with contact lens wear, such as conjunctivitis and red-eye syndrome, have been attributed to improper hygiene and noncompliance with recommended lens care procedures. Proper care of contact lenses requires the wearer to follow a precise lens care regimen, which normally includes cleaning, rinsing, and disinfection.

In general, there are two ways to disinfect hydrogel contact lenses. One is thermal disinfection, which was the first method used; the other is chemical disinfection. The advantages of thermal disinfection include short cycle times, efficacy against a variety of vegetative microorganisms, and low risk of ocular reaction when unpreserved saline is used. On the other hand, it may not be compatible with all lenses types,

and repeated heating may change the physical parameters of lenses. Furthermore, denatured proteins adhering to the lenses because of heating cause an allergic reaction in some individuals. In an attempt to provide a more convenient, less destructive regimen than thermal disinfection, chemical systems were introduced. These contain antimicrobial agents that interact with microorganisms; each agent has a unique chemical structure and reactive groups that induce varying degrees of microbial damage. This system, which does not use heat, is termed cold disinfection. Multipurpose solutions (MPSs), a type of cold disinfection, were introduced recently. MPSs that can be used for cleaning, rinsing, disinfecting, and storing have become as popular as cold disinfection. The convenience of MPSs leads to high compliance. On the other hand, in contrast to other care solutions, the eye, especially the cornea, is exposed directly to MPS. Although the numbers of those who use MPSs have been increasing, there are few exact criteria to evaluate whether the MPSs have severe effects on the cornea.

Gap junctions are membrane channels that permit the transfer of ions and small molecules between neighboring cells.<sup>1–3</sup> These channels are composed of hexameric hemichannels, or connexons, which are attached to the con-

Correspondence to: T. Tsuchiya, Division of Medical Devices, National Institute of Health Sciences, 1-18-1 Kamiyoga, Setagaya-ku, Tokyo 158-8501, Japan  
Contract grant sponsor: Japan Health Science Foundation

TABLE I. Main Ingredients of Three Types of MPS

Chemical Disinfectants	Main Ingredients
MPS-A	Polyhexamethylenebiguanide, poloxamine
MPS-B	Polyhexamethylenebiguanide
MPS-C	Polidronium chloride

nexon in the plasma membrane of neighboring cells. Gap junctional intercellular communication (GJIC) is suggested to play an important role in cell growth, cell differentiation, and tissue homeostasis. Moreover, GJIC inhibition by chemical substrates and some materials has been recognized as being involved in tumorigenesis.<sup>4,5</sup> The gap junction is composed of connexin, which is a membrane protein. On the cornea, connexin-43 is expressed in epithelial cells, keratocytes, and endothelial cells.<sup>6-9</sup>

Previous studies have assessed three types of MPS with the use of a V79 MC assay,<sup>10</sup> which evaluates the inhibitory activity of the intercellular gap-junctional communication that plays important roles in tissue homeostasis with the use of the V79 cell line, as this assay is a more sensitive method to evaluate contact lens care solutions. The results indicated that one MPS had an inhibitory action on GJIC. Moreover, the surfactant, poloxamine, which is one of the ingredients, had an inhibitory action on GJIC. In the present study, the effects of MPS on gap-junctional intercellular communication were assessed by SLDT assay, which evaluates the GJIC. Moreover, an attempt was made to conduct an immunohistochemical method to focus on connexin-43, which is a major protein-constituting gap junctional channel of these cells, in rabbit corneal keratocytes.

## MATERIALS AND METHODS

### Materials

Three types of multipurpose solution (MPS-A, MPS-B, MPS-C) were investigated in this study. Their main ingredients are shown in Table I. PHMB was obtained from Avecia Co, Ltd. Poloxamine and poloxamer-407 were obtained from BASF. Lucifer Yellow was purchased from Molecular Probes, Inc.

### Cell Culture

The standard medium of ME10 in this experiment was Eagle's Minimal Essential Medium (MEM) (Nissui Pharmaceutical Co., Ltd., Japan) containing 10 vol% fetal calf serum (Sanko Junyaku Co., Ltd., Japan).

Rabbit corneal keratocytes (RC4) were obtained from the RIKEN gene bank. They were thawed and cultured in ME10 medium in 25-cm<sup>2</sup> culture flasks (Corning) in incubators under standard conditions (37 °C, 5% CO<sub>2</sub>, 95% relative humidity). The cells were fed every 2 days with ME10 and subcultured in 75-cm<sup>2</sup> culture flasks (Corning).

### Scrape Loading and Dye Transfer Assay (SLDT Assay)

GJIC was assessed by scrape loading and dye transfer assay (SLDT assay).<sup>11,12</sup> As test solutions, appropriate concentrations of MPSs or their ingredients diluted by ME10 were used. After confluent RC4 cells were treated in 35-mm<sup>2</sup> dishes with test solutions, they were washed with phosphate-buffered saline containing CaCl<sub>2</sub> and MgCl<sub>2</sub> [PBS(+)]. Ten scrapes were made with a steel-blade scalpel and the cells were incubated with 0.2% Lucifer Yellow solution for 5 min under standard conditions (37 °C, 5% CO<sub>2</sub>, 95% relative humidity). The cells were then washed with PBS(+).

The distance that Lucifer Yellow had traveled through gap junctions was observed and recorded with an inverted fluorescent microscope equipped with a camera. The distance was measured at 30 points per dish and the average value was calculated. Each value was analyzed statistically with Tukey(a) multiple-comparison test. Each experiment was performed in triplicate.

### Western Blotting

First, confluent cultures of RC4 cells were treated with ME10 containing 0.065 vol% MPS-A for 30 min under standard conditions (37 °C, 5% CO<sub>2</sub>, 95% relative humidity). Then, they were quickly washed with ice-cold PBS(+). The cells were lysed by treating with 2% SDS containing 1-mM phenylmethyl sulfonyl fluoride (PMSF), 50-mM NaF, and 100-mM Na<sub>3</sub>VO<sub>4</sub>. These cell lysates were centrifuged (10,000 rpm) at 4 °C for 20 min to remove insoluble material. The protein concentration of the lysates was determined with BCA assay (Pierce, IL). The proteins were separated by 8% SDS polyacrylamide gels and transferred to PVDF membrane at 120 V for 30 min. Connexin-43 was detected with the use of anti-connexin-43 monoclonal antibody (anti-CX43 Chemicon, CA), followed by incubation with horseradish peroxidase (HRP)-conjugated secondary antibody and detection with ECL chemiluminescent detection reagent (Amersham Pharmacia Biotech UK Ltd., UK).<sup>13</sup>

### Balb 3T3 Two-Steps Cell-Transformation Assay

Balb 3T3 clone A3-1-1-1 cells were provided by Dr. Kuroki, University of Tokyo. The cells were cultured in ME10 in incubators under standard conditions (37 °C, 5% CO<sub>2</sub>, 95% relative humidity). For the cell-transformation assay, 10<sup>4</sup> cells were plated per 60-mm tissue-culture dish; 15 dishes were used for each point in all cell-transformation assays. After 24 h, 0.5-mg/ml 3-methylcholanthrene (MCA), a positive control, was added to culture medium, and 72 h later the cultures were washed with fresh medium and incubated in ME10 for 3 days. The cells were subsequently cultured in normal medium until the end of the culture. The medium was changed twice per week for 6 weeks. In the case of the assay for MPS, the medium was changed following a procedure similar to that described above, except there was addition of MCA. The cells were fixed and stained with 5% Giemsa solution. The types of transformed focus were determined

TABLE II. Inhibitory Potentials of MPS-A, MPS-B, and MPS-C in V79 MC Assay

Chemical Disinfectants	MC Assay <sup>a</sup>		Cytotoxicity IC50 <sup>b</sup>
	Result	Lowest Effective Concentration	
MPS-A	+	0.625 vol%	1.8 vol%
MPS-B	-	-	>10 vol%
MPS-C	-	-	>10 vol%

<sup>a</sup> The results of MC assay were obtained from a previous study (Reference 10). +, the inhibitory activities were observed in noncytotoxic concentrations; -, no inhibitory activities.

<sup>b</sup> IC50: the concentration that suppressed colony formation to 50% of the control value.

under a dissecting microscope. Foci that showed a clearly transformed phenotype were counted as described in the report of the IARC/NCI/EPA Working Group.<sup>14</sup> Each finding (the average number of transformed foci) was statistically analyzed with Tukey's (a) multiple-comparison test.

## RESULTS AND DISCUSSION

In previous studies, three types of multipurpose solutions were investigated with the use of the cytotoxicity test and the MC assay.<sup>10</sup> The MC assay is a method used to clarify the inhibitory activity of gap junctional intercellular communication. The method was described previously,<sup>15,16</sup> with results as shown in Table II. The IC50 value of MPS-A was approximately 1.8 vol%. On the other hand, those of MPS-B and MPS-C were greater than 10 vol%. In the MC assay, MPS-A inhibited GJIC at concentrations ranging from 0.625 vol% (lowest effective inhibitory concentration) to 1.25 vol%, whereas on MPS-B and C no inhibitory activities were observed. The order of the strength of MC assay was therefore judged to be MPS-A > MPS-B and MPS-C. To analyze what caused the inhibitory activities of MPS-A, the main ingredients of MPS-A, PHMB and poloxamine, were evalu-

TABLE III. Inhibitory Potentials of Poloxamine, PHMB, and Poloxamer-407 in V79 MC Assay

Chemical Substrate	MC Assay <sup>a</sup>		Cytotoxicity IC50 <sup>b</sup>
	Result	Lowest Effective Concentration	
Poloxamine	+	0.125%	0.4%
PHMB	-	-	1.2 ppm
Poloxamer-407	-	-	0.4%

<sup>a</sup> The results of MC assay were obtained from a previous study (Reference 10). +, the inhibitory activities were observed in noncytotoxic concentrations; -, no inhibitory activities.

<sup>b</sup> IC50: The concentration that suppressed colony formation to 50% of the control value.

ated with the use of a cytotoxicity test and an MC assay. At the same time, poloxamer-407, which also belongs to the surfactant of Pluronic acid was also evaluated. The results of the cytotoxicity test and MC assay are shown in Table III. The IC50 value of PHMB was approximately 1.2 ppm, and those of poloxamine and poloxamer 407 were approximately 0.4% each. Poloxamine inhibited GJIC at concentration ranging from 0.125% (the lowest effective inhibitory concentration) to 0.25%, while on PHMB no inhibitory activities were observed. This result suggested that the inhibitory activity observed in MPS-A was caused by poloxamine. Interestingly, no inhibitory action was observed in poloxamer-407, although poloxamer-407 has a comparable cytotoxicity to poloxamine. Because the conventional cytotoxicity test was not able to detect the difference between poloxamine and poloxamer-407, this MC assay is suitable for the screening of ingredients of MPSs.

Then an *in vitro* assay of GJIC was conducted by SLDT assay with the use of using RC4. The SLDT assay is a method to evaluate the GJIC by the distance of dye migration through the gap junction. The inhibitory action on GJIC could be detected by measuring the distance of dye (Lucifer yellow) migration through gap junctions (Figure 1). If there is an inhibitory action on GJIC, the distances of dye transfer de-

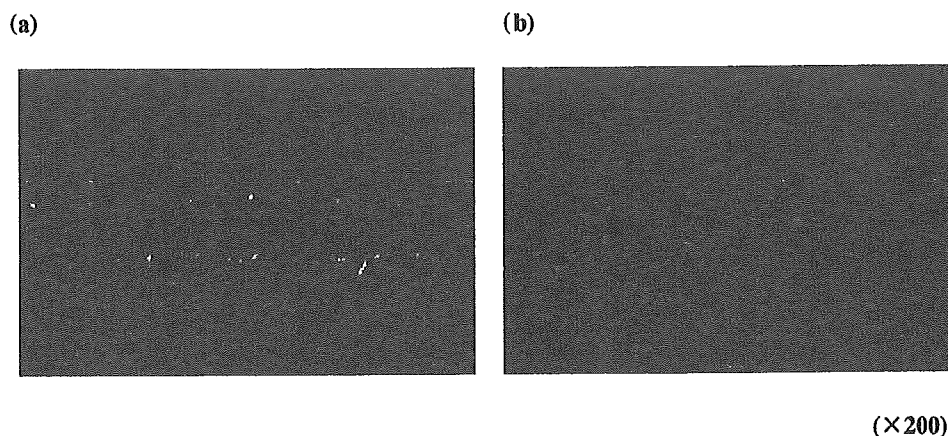
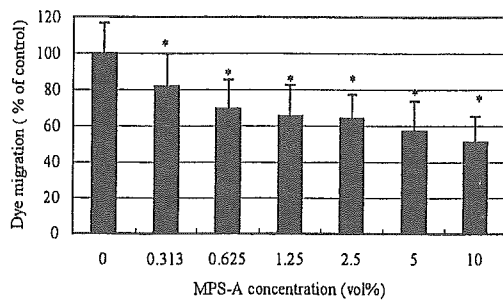
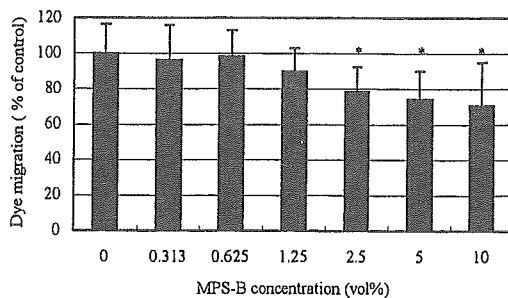


Figure 1. The image of SLDT assay. (a) Example where no inhibitory action was observed. (b) Example where inhibitory action was observed.

(a) MPS-A



(b) MPS-B



(c) MPS-C

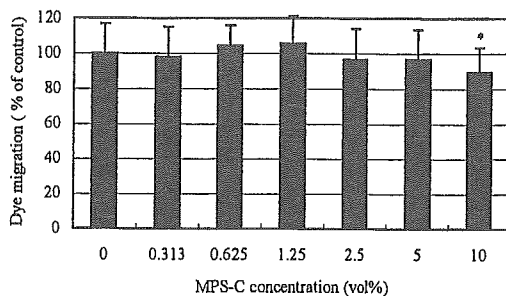
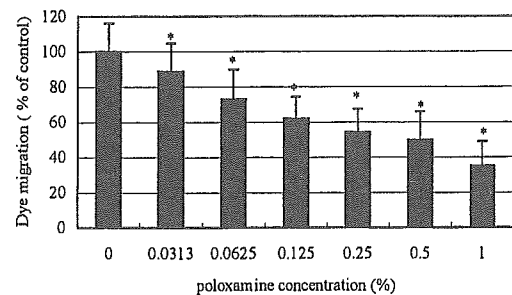


**Figure 2.** Dose-related inhibition of GJIC in RC4 cells treated with three types of MPS. (a) MPS-A, (b) MPS-B, (c) MPS-C. All data are expressed as the mean  $\pm$  standard deviation of 30 determinations and treated statistically with Tukey's(a) multiple-comparison test. \* $p < 0.01$ , significant difference in comparison with control.

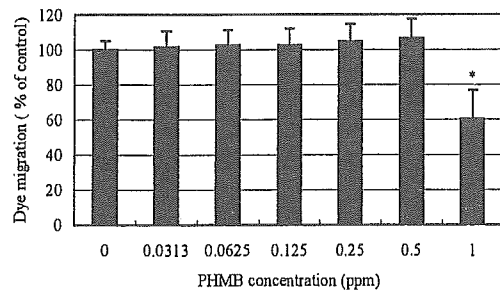
crease. First the concentration-dependent inhibition of MPSs were evaluated. These results are shown in Figure 2. After 24-h incubation under standard conditions, a dose-dependent inhibition was observed in all tested MPS. Especially for MPS-A, the inhibition was observed from 0.3125 vol% to a maximum at 10 vol%, revealing a 50% decrease. MPS-B produced dose-dependent inhibition from 2.5 vol% to a maximum at 10 vol%, compared with nontreatment cells [Tukey's(a) multiple-comparison test;  $p < 0.01$ ]. There was an inhibitory action of GJIC in MPS-C at 10 vol% compared with the nontreatment cells [Tukey's(a) multiple-comparison test;  $p < 0.01$ ]. Compared with MC assay, SLDT was more sensitive for the detection of inhibitory action on GJIC.

Second, the concentration-dependent inhibitions of poloxamine, PHMB, and poloxamer-407 were evaluated. These results are shown in Figure 3. After 24-h incubation under standard conditions, a dose-dependent inhibition was observed in poloxamine. It was observed from 0.03125% to a maximum at 1%, revealing a 50% decrease, whereas PHMB was not in its noncytotoxic concentration, compared with the nontreatment cells [Tukey's(a) multiple-comparison test;  $p < 0.01$ ]. These results coincided with those of the MC assay, so it strongly suggesting that the inhibitory activity observed in MPS-A was caused by poloxamine. Moreover, a difference between poloxamine and poloxamer-407 in the method of

(a) poloxamine



(b) PHMB



(c) poloxamer407

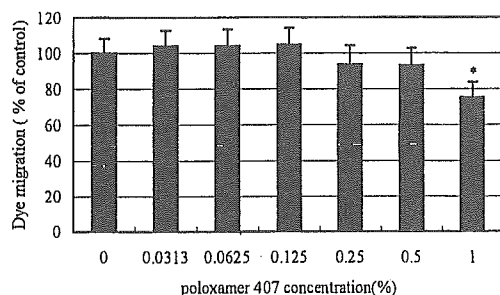
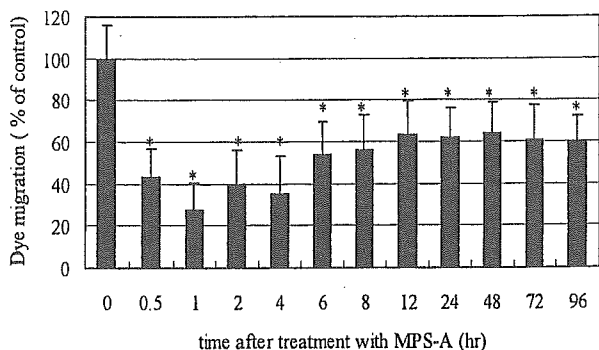


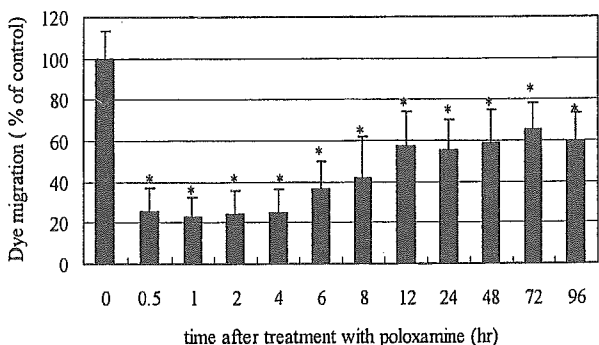
**Figure 3.** Dose-related inhibition of GJIC in RC4 cells treated with poloxamine, PHMB, and poloxamer-407. (a) Poloxamine, (b) PHMB, (c) poloxamer-407. All data are expressed as the mean  $\pm$  standard deviation of 30 determinations and treated statistically with Tukey's(a) multiple-comparison test. \* $p < 0.01$ , significant difference in comparison with control.



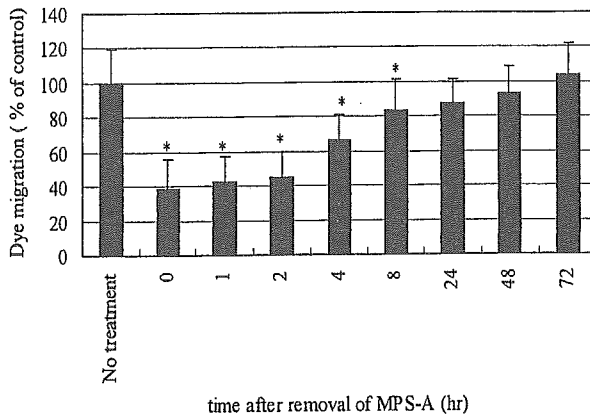
(a) MPS-A (0.625 vol%)



(b) poloxamine (0.125%)



(a) 1 hour



(b) 24 hour

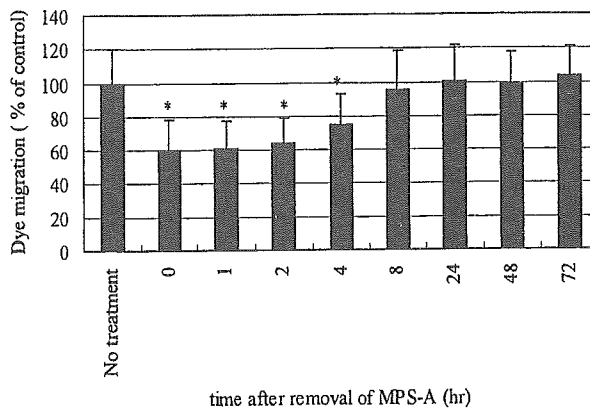


**Figure 4.** Time course of GJIC in RC4 cells after treatment with MPS-A and poloxamine for up to 96 h. (a) MPS-A, (b) poloxamine. All data are expressed as the mean  $\pm$  standard deviation of 30 determinations and treated statistically with Tukey's(a) multiple-comparison test. \* $p < 0.01$ , significant difference in comparison with control.

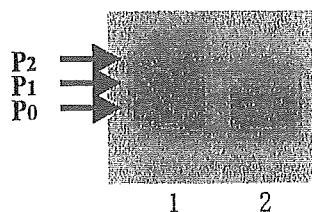
influencing on GJIC was suggested. These results also coincided with those of the MC assay.

Time-dependent GJIC inhibition was assessed after RC4 cells were treated with ME10 containing 0.625 vol% MPS-A or 0.125% poloxamine (Figure 4). In this experiment, confluent cultures of RC4 cells were treated with MPS-A or poloxamine under standard conditions. After that, the distance of dye migration was measured at appropriate times. (0–96 h after treatment). In MPS-A, an apparent inhibition of approximately 40% was observed at 30 min, and then GJIC

**Figure 5.** Time course of recovery of GJIC in RC4 cells after removal of MPS-A for up to 72 h. (a) 1-h treatment with MPS-A, (b) 24-h treatment with MPS-A. All data are expressed as the mean  $\pm$  standard deviation of 30 determinations and treated statistically with Tukey's(a) multiple-comparison test. \* $p < 0.01$ , significant difference in comparison with no treatment of control.

was gradually returned to 60% at 8 h, but the GJIC was not completely restored to the initial level after 8 h [Tukey's(a) multiple-comparison test;  $p < 0.01$ ]. In poloxamine, similar inhibitory action on GJIC was observed, and GJIC was not restored completely [Tukey's(a) multiple-comparison test;  $p < 0.01$ ].

(a) 30 min



(b) 24 hour

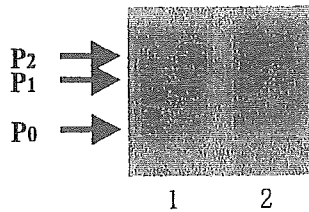


**Figure 6.** Western blotting of connexin-43 in RC4 cells treated with MPS-A. (a) 1-h treatment with MPS-A, (b) 24-h treatment with MPS-A. Connexin-43 is phosphorylated at least twice.<sup>21</sup> This results in three species<sup>21</sup> of connexin-43, which can be detected by Western blot ( $P_0$ ,  $P_1$ ,  $P_2$ ).<sup>21</sup>  $P_0$  is not phosphorylated, and  $P_1$  and  $P_2$  are phosphorylated.<sup>21</sup>

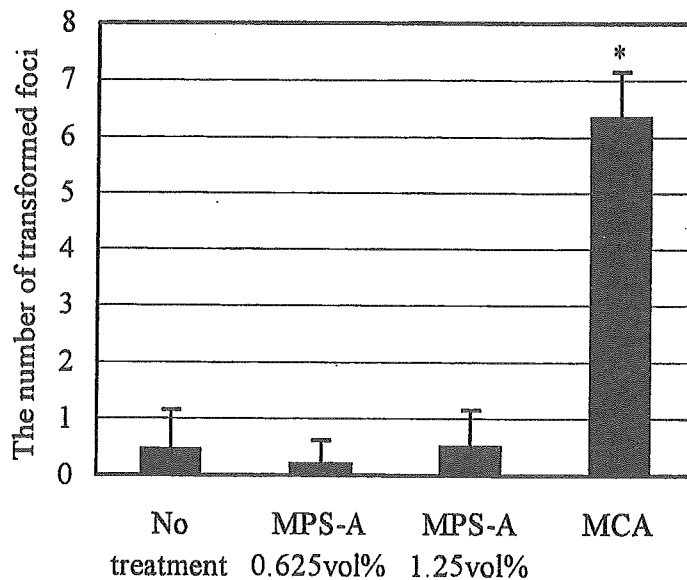
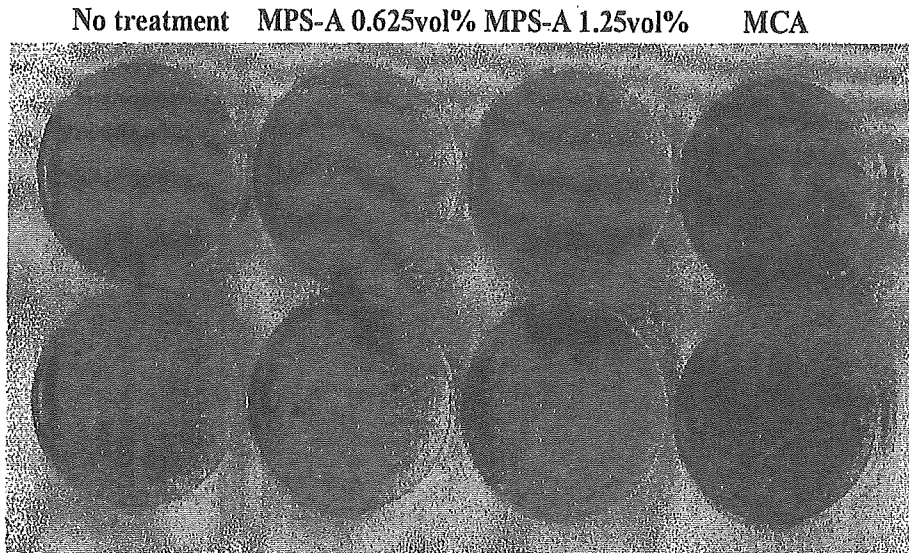


**Figure 7.** Two-stage Balb3T3 cell transformation test for MPS-A. Each bar represents the mean  $\pm$  standard deviation of 15 determinations in graph. Transformed foci were deeply stained by Giemsa staining, as shown in the dishes (upper photos). All data are expressed as the mean  $\pm$  standard deviation of 15 determinations and treated statistically with Tukey's (a) multiple-comparison test. \* $p < 0.05$ , significant difference in comparison with no treatment of control. Experiments were repeated at least two times.

Then, the time course for recovery from MPS-A-induced inhibition of GJIC was examined (Figure 5). In this experiment, confluent cultures of RC4 cells were treated with MPS-A (0.625 vol%) or poloxamine (0.125%) for 1 h under standard conditions. After that, the medium was replaced with fresh ME10 and the distance of dye migration was measured at appropriate times (0–72 h after treatment). As a result, the recovery of GJIC was time dependent and reached former levels in 24 h [Tukey's(a) multiple-comparison test;  $p < 0.01$ ]. The time course of recovery after exposure for

24 h is also shown in Figure 5. Similarly, time-dependent restoration was observed after 4 h, and complete recovery was established after approximately 24 h [Tukey's(a) multiple-comparison test;  $p < 0.01$ ]. These results showed that the method of inhibition induced by MPS-A was reversible.

Western-blotting analysis was conducted for connexin-43, which is a major protein constituting the gap junctional channels of these cells, to examine whether MPS-A caused changes in the amounts of this protein, in addition to the degree of its phosphorylation after treatment of RC4 cells

with MPS-A (Figure 6). The three typical bands ( $P_0$ ,  $P_1$ ,  $P_2$ ) of connexin-43 corresponding to three forms of connexin-43 that have been identified in other cells, were detected in untreated RC4 cells. They were separated according to the degree of phosphorylation state; the  $P_0$  represents nonphosphorylated connexin-43, and  $P_2$  represents a much higher phosphorylated state than  $P_1$ . After 30 min of incubation with 0.625 vol% MPS-A in RC4 cells under standard conditions, the total level of connexin-43 in the cells was reduced. Importantly, decreasing amounts of  $P_2$  were observed compared with the amounts in control cells. After 24 h incubation, the total level of connexin-43 was approximately restored and the amounts of  $P_2$  were also restored. Therefore, it was suggested that this short-time decrease in the amount of connexin-43 was ascribed to the inhibitory action on GJIC. Moreover, the inhibitory action might be induced by the change in connexin-43 to the dephosphorylated form, such as the  $P_2$  level, to  $P_1$  or  $P_0$ . It was reported that the phosphorylated state of connexin-43 is important for its accurate assembly and distribution in cells.<sup>4</sup> Probably, connexin-43 on RC4 was not phosphorylated to the  $P_2$  level by MPS-A exposure, so that the gap junction could not assemble, which was ascribed to the inhibitory action on GJIC. To clarify this, the localization of connexin-43 is currently being evaluated by immunostaining.

The results in the present study supported the idea that the change in connexin-43 expression is the major cause of the change in GJIC function on the cornea when the cells were exposed to MPS-A. The method of the inhibitory action in RC4 was reversible, but it took approximately 24 h for the GJIC to be restored completely. Many contact lens users typically wear contact lenses for over 12 h, and in some cases hydrogel contact lenses swell or absorb the ingredients of MPS-A. Therefore, there might be a situation that some MPS-A or its ingredient remains on the surface of contact lenses, which suggests that the corneas of wearers are exposed directly to them. In this case, MPS-A or its ingredients might cause disorder to the GJIC on the cornea, and so the phenomenon, which is always a disorder of the homeostasis of the cornea, is in a stationary state. It is possible that this state may lead to poor resistance for diseases. The finding that several diseases originated from the lack or damage of connexin<sup>17</sup> supports this kind of risk. In addition, recent immunohistochemical and immunoblotting studies showed that there was less connexin-43 in rat corneas exposed to MPS-A than in cornea exposed to MPS-B and C *in vivo* (data not shown). It was suggested that there is a disorder of the homeostasis of the cornea exposed to MPS-A *in vivo*, because it was suggested that the quantity and function of the gap junction is linked to the abundance of connexin-43. It is possible that the same phenomenon occurs on the corneas of humans (MPS-A users).

To study the tumor activity of MPS-A, a Balb3T3 two-stage cell transformation assay was conducted (Figure 7). No significant difference was found between ME10 containing MPS-A 1.25 vol%, 0.625 vol%, and negative controls (ME10 alone) [Tukey's(a) multiple-comparison test;  $p > 0.05$ ].

These results suggested that the tumor-promoting potency of MPS-A is low, compared with positive controls (MCA) or phorbol esters that are well known as tumor-promoting agents.<sup>18</sup> However, there is definitely a disorder of GJIC on cells exposed to MPS-A, which causes a dysfunction to the homeostasis of the cornea. Recently, it was reported that disruption of connexin leads to cataractogenesis in mice.<sup>19</sup> So, it is possible that exposing the cornea to MPSs, which inhibit GJIC, can have a severe influence on the homeostasis of the cornea and induce cataractogenesis or other diseases.<sup>20</sup>

The present study tried to introduce methods to evaluate the effects on GJIC as a criterion for safety for the cornea. These methods could detect inhibitory activities of GJIC at non-cytotoxic concentrations. Compared with previous methods, this one is thought to be more suitable for evaluating the long-term safety of MPS.

The authors thank Yuki Suita for her technical assistance.

## REFERENCES

1. Yamasaki H, Mesnil M, Omori Y, Mironov N, Krutovskikh V. Role of blocked gap junctional intercellular communication in non-genotoxic carcinogenesis. *Toxicol Lett* 1995;82-83:701-706.
2. Bennett MV, Barrio LC, Bargiello TA, Spray DC, Hertzberg E, Saez JC. Gap junctions: New tools, new answers, new questions. *Neuron* 1991;6:305-320.
3. Kumar NM, Gilula NB. The gap junction communication channel. *Cell* 1996;84:381-388.
4. Yamasaki H. Role of disrupted gap junctional intercellular communication in detection and characterization of carcinogens. *Mutat Res* 1996;365:91-105.
5. Tsuchiya T. Detection of tumor-promoting activities in biomaterials using *in vitro* cell culture methods. *Kobunshi Ronbunshu* 1998;55:314-322.
6. Dong Y, Roos M, Gruijters T, Donaldson P, Bullivant S, Beyer E, Kistler J. Differential expression of two gap junction proteins in corneal epithelium. *Eur J Cell Biol* 1994;64:95-100.
7. Matic M, Petrov IN, Rosenfeld T, Wolosin JM. Alterations in connexin expression and cell communication in healing corneal epithelium. *Invest Ophthalmol Vis Sci* 1997;38:600-609.
8. Petridou S, Masur SK. Immunodetection of connexins and cadherins in corneal fibroblasts and myofibroblasts. *Invest Ophthalmol Vis Sci* 1996;37:1740-1748.
9. Joyce NC, Harris DL, Zieske JD. Mitotic inhibition of corneal endothelium in neonatal rats. *Invest Ophthalmol Vis Sci* 1998;39:2572-2583.
10. Sumide T, Tsuchiya T. Evaluation of chemical disinfectants for hydrogel contact lenses by metabolic cooperation assay. *J Jpn Soc Biomater* 2001;119:93-97.
11. El-Fouly MH, Trosko JE, Chang CC. Scrape-loading and dye transfer. A rapid and simple technique to study gap junctional intercellular communication. *J Exp Cell Res* 1987;168:422-430.
12. Park JU, Tsuchiya T. Increase in gap-junctional intercellular communications (GJIC) of normal human dermal fibroblasts (NHDF) on surfaces coated with high-molecular-weight hyaluronic acid (HMW HA). *J Biomed Mater Res* 2002;60:541-547.
13. Ichikawa A, Tsuchiya T. Reversion of transformed phenotype of polyetherurethane-induced tumor cells by Cx43 transfection. *Animal Cell Technol Basic Appl Aspects* 2002;12:269-273.

14. IARC/NCI/EPA Working Group. Cellular and molecular mechanisms of cell transformation and standardization of transformation assays of established cell lines for the prediction of carcinogenic chemicals: Overview and recommended protocols. *Cancer Res* 1985;45:2395-2399.
15. Yotti LP, Chang CC, Trosko JE. Elimination of metabolic cooperation in Chinese hamster cells by a tumor promoter. *Science* 1979;206:1089-1091.
16. Tsuchiya T, Hata T, Nakamura A. Studies on the tumor-promoting activity of biomaterials: Inhibition of metabolic cooperation by polyetherurethane and silicone. *J Biomed Mater Res* 1995;29:113-119.
17. Donaldson P, Eckert R, Green C, Kistler J. Gap junction channels: New roles in disease. *Histol Histopathol* 1997;12:219-231.
18. Yamasaki H, Krutovskikh V, Mesnil M, Tanaka T, Zaidan-Dagli ML, Omori Y. Role of connexin (gap junction) genes in cell growth control and carcinogenesis. *C R Acad Sci III* 1999;322:151-159.
19. Gong X, Li E, Klier G, Huang Q, Wu Y, Lei H, Kumar NM, Horwitz J, Gilula NB. Disruption of alpha3 connexin gene leads to proteolysis and cataractogenesis in mice. *Cell* 1997;91:833-843.
20. Suzuki K, Tanaka T, Enoki M, Nishida T. Coordinated reassembly of the basement membrane and junctional proteins during corneal epithelial wound healing. *Invest Ophthalmol Vis Sci* 2000;41:2495-2500.
21. Trosko JE, Ruch RJ. Cell-cell communication in carcinogenesis. *Frontiers Biosci* 1998;3:208-236.



## Osteoblast Differentiation and Apatite Formation on Gamma-Irradiated PLLA Sheets

Kazuo Isama<sup>a</sup> and Toshie Tsuchiya<sup>b</sup>

Division of Medical Devices, National Institute of Health Sciences,  
Kamiyoga 1-18-1, Setagaya-ku, Tokyo 158-8501, Japan

<sup>a</sup>isama@nihs.go.jp, <sup>b</sup>tsuchiya@nihs.go.jp

**Keywords:** Poly(L-lactide), gamma-ray irradiation, osteoblast differentiation, apatite formation.

**Abstract.** The effects of the  $\gamma$ -irradiated PLLA on the osteoblasts and apatite formation were investigated *in vitro*. The PLLA sheet was  $\gamma$ -ray irradiated at the dose of 10, 25 or 50 kGy. The mouse osteoblast-like MC3T3-E1 cells and normal human osteoblast NHOst cells were micromass cultured on the PLLA sheet for 2 weeks, and then the proliferation and differentiation of the cells were determined. The proliferations of MC3T3-E1 and NHOst cells hardly changed with increasing irradiation dose. However, the differentiations of MC3T3-E1 and NHOst cells increased with irradiation dose. On the other hand, the surface of the PLLA sheet after soaking in the medium without the cells was characterized by SEM, EDX, FT-IR and XPS. The hydroxyapatite was formed on the surface of the PLLA sheet after soaking, and the amount of hydroxyapatite increased with irradiation dose. In summary, the  $\gamma$ -irradiated PLLA increased the differentiation of osteoblasts and also increased apatite-forming ability even without the osteoblasts. The osteoblast differentiation was enhanced well in the apatite formation on the surface of PLLA after the  $\gamma$ -irradiation.

### Introduction

Poly(L-lactide) (PLLA) has been well reported on a good osteocompatibility *in vivo* and *in vitro*. The  $\gamma$ -ray sterilized PLLA sample was implanted *in vivo*, and newly bone was formed around the PLLA implant [1]. It was not clear whether there was the effect of  $\gamma$ -irradiation on the formation of newly bone in this result. However, it was the fact that  $\gamma$ -irradiation decreased the molecular weight and mechanical strength of PLLA [2]. On the other hand, PLLA fibers formed bone-like apatite in a simulated body fluid [3]. It was reported that the apatite layer formed on the bioactive glass increased the attachment and initial proliferation of osteoblasts [4]. If the apatite-forming ability of PLLA is increased by  $\gamma$ -irradiation, there may be a good influence on osteoblasts cultured on the irradiated PLLA. Therefore, we clarified the effects of the  $\gamma$ -irradiated PLLA sheet on the osteoblasts and apatite formation *in vitro*.

### Materials and Methods

**Materials.** PLLA sheet with 0.3 mm thickness (Shimadzu Co., Japan) was  $\gamma$ -ray irradiated at the dose of 10, 25 or 50 kGy using <sup>60</sup>Co as the radiation source. The weight average molecular weight (Mw) of the unirradiated PLLA was 271,000 and the Mw's of the irradiated PLLA's at the dose

of 10, 25 and 50 kGy were respectively 195,000, 142,000 and 95,000 by GPC.

**Micromass Culture of Osteoblasts.** Mouse osteoblast-like MC3T3-E1 cells (RIKEN Cell Bank, Japan) and normal human osteoblast NHOst cells (Clonetics Corporation, MD, USA) were grown in alpha minimum essential medium ( $\alpha$ -MEM) supplemented with 20% fetal bovine serum. The PLLA sheet was cut into 14.0 mm diameter disk and laid in a 24-well dish. The 20  $\mu$ l of cell suspension ( $2 \times 10^6$  cells/ml) was delivered on the disk. After the cells were attached on the disk, 1 ml of the complete medium that contained 10 mM disodium  $\beta$ -glycerophosphate in the culture medium was added. The complete medium was changed three times a week, and the cells cultured for 2 weeks in a 37°C humidified atmosphere of 5% CO<sub>2</sub>.

**Proliferation Assay.** The number of the cells cultured on the PLLA sheet was determined by WST-8 assay [5]. Moreover, the protein and DNA contents of the cell lysate were measured by the Lowry method and the fluorescence assay using Hoechst 33258 dye, respectively [5].

**Differentiation Assay.** The calcium depositions of the cell cultures were stained by alizarin red S, and the areas stained dark-red were measured using the program Scion Image (Scion Co., MD, USA) [5]. The calcification was calculated as the normalized area in the cell number. Moreover, the collagen synthesis was evaluated by the hydroxyproline content of the cell lysate, and ALP activity of the cells was measured using *p*-nitrophenylphosphate as a substrate [5].

**Soaking in the Medium.** The PLLA sheet was cut into 14.0 mm diameter disk and laid in a 24-well dish. The complete medium of 1 ml was added without the cells. Then, the dish was stored in a 37°C humidified atmosphere of 5% CO<sub>2</sub>, and the complete medium was changed three times a week. After soaking for 2 weeks, the PLLA disk was washed in deionized water five times quickly and dried in a silica gel desiccator.

**Surface Analysis.** The surface of the PLLA sheet after soaking in the complete medium without the cells was characterized by SEM, EDX, FT-IR and XPS according to the conventional methods.

## Results

**Proliferation of Osteoblasts Cultured on the PLLA Sheet.** The cell number of MC3T3-E1 cells cultured on the PLLA sheet did not change with increasing irradiation dose (Fig. 1a). The protein and DNA contents of the cells also did not change. The other side, the cell number (Fig. 1b),

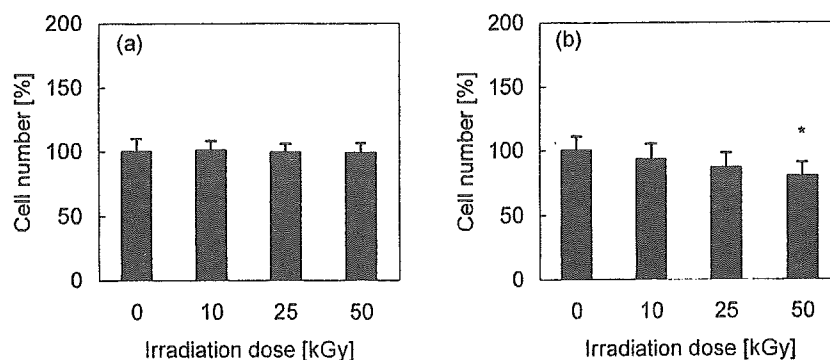


Fig. 1. The cell numbers of (a) MC3T3-E1 and (b) NHOst cells cultured on the  $\gamma$ -irradiated PLLA sheet.

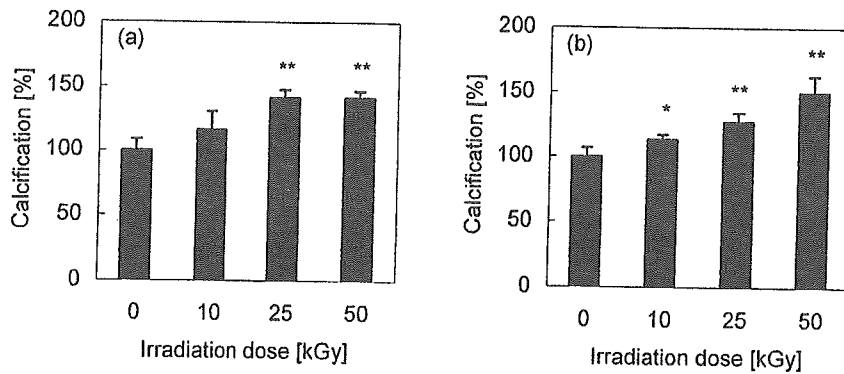


Fig. 2. The calcifications of (a) MC3T3-E1 and (b) NHOst cells cultured on the  $\gamma$ -irradiated PLLA sheet.

protein and DNA contents of NHOst cells cultured on the PLLA sheet slightly decreased with irradiation dose.

**Differentiation of Osteoblasts Cultured on the PLLA Sheet.** The calcification of MC3T3-E1 cells (Fig. 2a) and NHOst cells (Fig. 2b) remarkably increased with irradiation dose. The collagen synthesis and ALP activity of MC3T3-E1 and NHOst cells also increased as same as the calcification, respectively. The  $\gamma$ -irradiated PLLA remarkably promoted the differentiation of osteoblasts.

**Apatite Formation on the PLLA Sheet.** The SEM micrograph exhibited crystal particles on the surface of the PLLA sheet after soaking in the complete medium without the cells. The crystal particles were identified with hydroxyapatite by EDX, FT-IR and XPS spectra. The phosphate band in ATR/FT-IR spectra became strong with irradiation dose (Fig. 3). Moreover, the element ratios of calcium and phosphorus increased but that of carbon decreased with irradiation dose, in XPS analysis (Fig. 4). The amount of hydroxyapatite formed on the  $\gamma$ -irradiated PLLA sheet increased with irradiation dose.

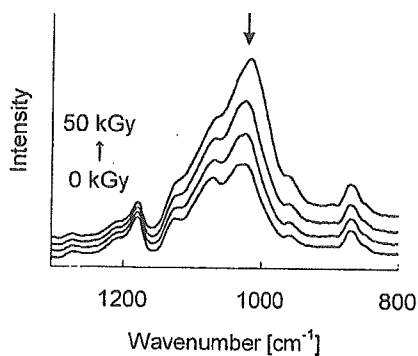


Fig. 3. The phosphate band of the  $\gamma$ -irradiated PLLA sheet after soaking in the medium.

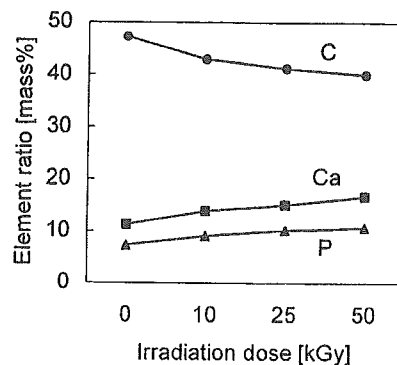


Fig. 4. The element ratios of calcium, phosphorus and carbon of the  $\gamma$ -irradiated PLLA sheet after soaking in the medium.

### Discussion

In the present study, the  $\gamma$ -irradiated PLLA hardly affected the proliferation but remarkably promoted the differentiation of osteoblasts. It was expected that the low molecular weight PLLA eluted to the medium, because the molecular weight of PLLA decreased by  $\gamma$ -irradiation. In our recent studies, the low molecular weight PLLA enhanced the differentiation of MC3T3-E1 cells but inhibited that of NHOst cells [6, 7]. The present results, which the differentiations of MC3T3-E1 and NHOst cells both increased on the  $\gamma$ -irradiated PLLA sheet, would not be caused by the low molecular weight PLLA. The surface of the  $\gamma$ -irradiated PLLA should good influence on the differentiation of osteoblasts.

On the other hand, the  $\gamma$ -irradiation increased the apatite-forming ability of the PLLA sheet. Tanahashi and Matsuda reported that some negatively charged groups such as phosphate and carboxyl group strongly induced apatite formation in a simulated body fluid. They described that the apatite formation was initiated via calcium ion-absorption upon complexation with a negative surface-charged group [8]. In our study, the molecular weight of PLLA decreased with hydrolysis of ester bonds by  $\gamma$ -irradiation [2]. Therefore, the amount of carboxyl group of the  $\gamma$ -irradiated PLLA would increase with irradiation dose, and the carboxyl group would promote the apatite-forming ability of the PLLA sheet.

Fujibayashi *et al.* compared *in vivo* bone ingrowth and *in vitro* apatite formation on  $\text{Na}_2\text{O-CaO-SiO}_2$  glasses. The quantities of newly bone formed on the glasses correlated with their apatite-forming abilities in simulated body fluid. They propose to evaluate the apatite-forming ability in order to confirm the *in vivo* bioactivity of biomaterials [9]. In our present study, the  $\gamma$ -irradiation enhanced the apatite-forming ability of the PLLA sheet, and then the  $\gamma$ -irradiated PLLA sheet promoted the differentiation of osteoblasts. The osteoblast differentiation should connect with the apatite formation on the  $\gamma$ -irradiated PLLA sheet.

In conclusion, the  $\gamma$ -irradiated PLLA hardly affected the proliferation but promoted the differentiation of osteoblasts with increasing irradiation dose. On the other hand, the hydroxyapatite was formed on the PLLA sheet in the medium, and the  $\gamma$ -irradiation enhanced apatite-forming ability of the PLLA. It was suggested that the connection between the osteoblast differentiation and apatite formation on the  $\gamma$ -irradiated PLLA sheets.

### References

- [1] T.E. Otto, P. Patka, H.J.Th.M. Haarman, C.P.A.T. Klein and R. Vriesde: *J. Mater. Sci. Mater. Med.* 5 (1994), 407-410.
- [2] K. Isama and T. Tsuchiya: *Bull. Natl. Inst. Health Sci.* 119 (2001), 61-64.
- [3] X. Yuan, A.F.T. Mak and J. Li: *J. Biomed. Mater. Res.* 57 (2001), 140-150.
- [4] N. Olmo, A.I. Martin, A.J. Salinas, J. Turnay, M. Vallet-Regi and M.A. Lizarbe: *Biomaterials* 24 (2003), 3383-3393.
- [5] K. Isama and T. Tsuchiya: *J. Biomater. Sci. Polymer Edn.* 13 (2002), 153-166.
- [6] K. Isama and T. Tsuchiya: *Biomaterials* 24 (2003), 3303-3309.
- [7] K. Isama, Y. Ikarashi and T. Tsuchiya: *BIO INDUSTRY* 19 (2002), 21-29.
- [8] M. Tanahashi and T. Matsuda: *J. Biomed. Mater. Res.* 34 (1997), 305-315.
- [9] S. Fujibayashi, M. Neo, H.M. Kim, T. Kokubo and T. Nakamura: *Biomaterials* 24 (2003), 1349-1356.